On the quest for chaotic attractors in hydrological processes: Additional information

Internal report

Demetris Koutsoyiannis

Department of Water Resources, Faculty of Civil Engineering, National Technical University of Athens, Heroon Polytechneiou 5, GR-157 80 Zographou, Greece (dk@itia.ntua.gr)

Abstract This report contains additional information for the paper *On the quest for chaotic attractors in hydrological processes*, including mathematical derivations and the complete studies with real world examples.

1. Theoretical investigation of correlation dimension of asymmetric processes

Let Y_n be a random process on discrete time n with all Y_n (n = 1, 2, …) independent identically distributed positive variables with distribution function $F(y)$ and density $f(y)$. We assume that $y > 0$ (as happens with all hydrological variables) and also $y < \xi$ where the upper bound ξ could be finite or infinite. We will study the correlation dimension for embedding dimension m = 1. We consider a partition of the y domain with scale ε. Applying equations (7) and (8) from Koutsoyiannis (2006) and observing that $p_i = F(i\,\varepsilon) - F((i-1)\varepsilon)$ we find

$$D_2 = \lim_{\varepsilon \to 0} \left\{ \frac{1}{\ln \varepsilon} \ln \sum_{i=1}^{\nu(\varepsilon, \xi)} [F(i\,\varepsilon) - F((i-1)\varepsilon)]^2 \right\} \tag{A1}$$

where $\nu(\varepsilon, \xi)$ is the smallest integer that is greater than or equal to ξ / ε. For small values of ε $F(i\,\varepsilon) - F((i-1)\varepsilon) = f(i\,\varepsilon)\,\varepsilon$ and therefore when $\varepsilon \to 0$,

$$D_2 = 1 + \lim_{\varepsilon \to 0} \left[\frac{1}{\ln \varepsilon} \ln \sum_{i=1}^{\nu(\varepsilon, \xi)} f^2(i\,\varepsilon)\,\varepsilon \right] \tag{A2}$$

Also, when $\varepsilon \to 0$,

$$\sum_{i=1}^{\nu(\varepsilon, \xi)} f^2(i\,\varepsilon)\,\varepsilon \to \int_0^{\xi} f^2(y)\,dy =: B \tag{A3}$$

Obviously, if B converges then $D_2 = 1$. This case is the most commonly met, since in most cases $f(y)$ has a finite value for the entire domain of y. If $f(y)$ is finite, B converges even if ξ is infinite. This is understood if we observe that in this case, there exists an $y_0 > 0$ so that $f(y) < 1$ for any $y > y_0$ and therefore $f^2(y) < f(y)$. Thus, the integral $f^2(y)$ in $[x_0, \infty)$ is finite, and since $f(y)$ is finite everywhere, the integral in $[0, \infty)$ will be finite, too. Consequently the limit in (A2) becomes zero and $D_2 = 1$.

Now we consider the case that B does not converge. There are two possible sufficient conditions that may lead to this case: $f(y)$ tends to ∞ either when y tends to 0 or when y tends to ξ where ξ is finite. We concentrate on the first condition, which is the most interesting as far as hydrological processes are concerned. In this case only the first term ($i = 1$) of the sum in (A1) is significant so that

$$D_2 = 2 \lim_{\varepsilon \to 0} \frac{\ln [F(\varepsilon)]}{\ln \varepsilon} \tag{A4}$$

Applying de l'Hôpital's rule twice we get

$$D_2 = 2 \lim_{\varepsilon \to 0} \frac{\varepsilon f(\varepsilon)}{F(\varepsilon)} = 2 + 2 \lim_{\varepsilon \to 0} \frac{\varepsilon f'(\varepsilon)}{f(\varepsilon)} \tag{A5}$$

where $f'(\,)$ is the derivative of $f(\,)$.

Now let us view a few examples. First we consider the Pareto distribution, in which

$$F(y) = (y / a)^{\kappa},\ f(y) = (\kappa / a)\ (y / a)^{\kappa - 1},\ f'(y) = (\kappa - 1)(\kappa / a^2)\ (y / a)^{\kappa - 2},\ 0 \le y \le a \tag{A6}$$

Here $\xi = a$. The integral B converges to $(\kappa^2 / a) / (2\,\kappa - 1)$ when $\kappa > 1/2$ and diverges when $\kappa < 1/2$. Therefore, for $\kappa > 1/2$, $D_2 = 1$, whereas for $\kappa < 1/2$,

$$D_2 = 2 + 2 \lim_{\varepsilon \to 0} \frac{(\kappa - 1)(\kappa / a^{\kappa})\ \varepsilon^{\kappa - 1}}{(\kappa / a^{\kappa})\ \varepsilon^{\kappa - 1}} = 2\,\kappa \tag{A7}$$

We note that the coefficient of skewness of this distribution is

$$C_s(\kappa) = \frac{2\ (1 - \kappa)\sqrt{2 + \kappa}}{(3 + \kappa)\sqrt{\kappa}} \tag{A8}$$

which means that the correlation dimension is smaller than 1 when the coefficient of skewness is greater than $C_s(1/2) = 0.639$.

In our second example we consider the gamma distribution, in which

$$f(y) = [1 / a\,\Gamma(\kappa)]\,(y/a)^{\kappa-1}\,e^{-y/a},\; f'(y) = [1/a^2\,\Gamma(\kappa)]\,(\kappa-1-y/a)\,(y/a)^{\kappa-2}\,e^{-y/a},\; y>0 \quad \text{(A9)}$$

The integral B converges to $\Gamma(\kappa - 1/2) / [2\sqrt{\pi}\,a)\;\Gamma(\kappa)]$ when $\kappa > 1/2$ and diverges when $\kappa < 1/2$. Therefore, for $\kappa > 1/2$, $D_2 = 1$, whereas for $\kappa < 1/2$,

$$D_2 = 2 + 2 \lim_{\varepsilon \to 0} \frac{[1/a^2\,\Gamma(\kappa)]\,\varepsilon\,(\kappa - 1 - \varepsilon/a)\,(\varepsilon/a)^{\kappa-2}\,e^{-\varepsilon/a}}{[1/a\,\Gamma(\kappa)]\,(\varepsilon/a)^{\kappa-1}\,e^{-\varepsilon/a}} = 2\,\kappa \quad \text{(A10)}$$

We note that the coefficient of skewness of this distribution is $C_s(\kappa) = 2/\sqrt{\kappa}$, which means that the correlation dimension is smaller than 1 when the coefficient of skewness is greater than $C_s(1/2) = 2.83$.

In our third example we consider the Weibull distribution, i.e.,

$$F(y) = 1 - \exp[-(y/a)^\kappa],\; f(y) = (\kappa/a)\,(y/a)^{\kappa-1}\exp[-(y/a)^\kappa]$$
$$f'(y) = (\kappa/a^2)\,[\kappa - 1 - (y/a)^\kappa]\,(y/a)^{\kappa-2}\exp[-(y/a)^\kappa],\; y>0 \quad \text{(A11)}$$

The integral B converges to $(\kappa/a)\,\Gamma(2 - 1/\kappa) / 2^{2-1/\kappa}$ when $\kappa > 1/2$ and diverges when $\kappa < 1/2$. Therefore, for $\kappa > 1/2$, $D_2 = 1$, whereas for $\kappa < 1/2$,

$$D_2 = 2 + 2 \lim_{\varepsilon \to 0} \frac{(\kappa/a^2)\,\varepsilon\,[\kappa - 1 - (\varepsilon/a)^\kappa]\,(\varepsilon/a)^{\kappa-2}\exp[-(\varepsilon/a)^\kappa]}{(\kappa/a)\,(\varepsilon/a)^{\kappa-1}\exp[-(\varepsilon/a)^\kappa]} = 2\,\kappa \quad \text{(A12)}$$

We note that the coefficient of skewness of this distribution is

$$C_s(\kappa) = \frac{2\,\Gamma^3(1+1/\kappa) - 3\,\Gamma(1+1/\kappa)\,\Gamma(1+2/\kappa) + \Gamma(1+3/\kappa)}{[\Gamma(1+2/\kappa) - \Gamma^2(1+1/\kappa)]^{3/2}} \quad \text{(A13)}$$

which means that the correlation dimension is smaller than 1 when the coefficient of skewness is grater than $C_s(1/2) = 6.62$.

2. Required sample size to estimate attractor dimensions

It is well known that the length of the confidence interval of the estimate of a probability p from a sample with relatively high size N for a confidence coefficient γ is $2\,z_{(1+\gamma)/2}\,[p\,(1-p)/N]^{0.5}$ where z_a is the a-quantile of the standard normal distribution. If c is the acceptable relative error in the estimation of p then

$$2\,z_{(1+\gamma)/2}\,[p\,(1-p)/N]^{0.5} = 2\,c\,p \quad \text{(A14)}$$

Solving for N, we find that the minimum sample size $N_{\min}$ that is required for estimating the probability p with confidence γ and acceptable relative error c is

$$N_{\min} = (z^2_{(1+\gamma)/2} / c^2)\,(1/p - 1) \tag{A15}$$

Now, if we replace p with the correlation sum (by its definition (12) in Koutsoyiannis, 2006, $C_2(\varepsilon, m)$ is an estimate of probability) and $N_{\min}$ with $N^2_{\min} / 2$ (since our sample in this case is composed of pairs of values), and also ignore 1 in the last term of (A15) (assuming that p is small so that $1/p$ is much larger than 1) we find that the minimum sample size required to estimate $C_2(\varepsilon, m)$ with confidence γ and acceptable relative error c is

$$N_{\min} = (z_{(1+\gamma)/2} / c)\,[2 / C_2(\varepsilon, m)]^{0.5} \tag{A16}$$

For a stochastic system, combining (A16) with (18) in Koutsoyiannis (2006) we find

$$N_{\min} = \sqrt{2}\,(z_{(1+\gamma)/2} / c)\,[C_2(\varepsilon, 1)]^{-m/2} \tag{A17}$$

If we replace ε in (A17) with $\overline{\varepsilon}$, the highest possible scale that suffices to accurately estimate the correlation dimension, we obtain equation (19) in Koutsoyiannis (2006).

For the choice of an acceptable relative error c we must investigate the relation of the relative error in estimating $C_2(\varepsilon, m)$ with that in estimating $d_2(\varepsilon, m)$, which is our final target. We assume that the local slope is calculated from two successive values of $C_2(\varepsilon, m)$, at scales ε_1 and $\varepsilon_2 = \alpha\,\varepsilon_1$, whose theoretical values are $C_2(\varepsilon_2, m) = \beta\,C_2(\varepsilon_1, m)$. We also assume that the empirical values depart from the theoretical ones by c each on opposite direction, i.e., $C'_2(\varepsilon_2, m) = (1 + c)\,C_2(\varepsilon_2, m)$ and $C'_2(\varepsilon_1, m) = (1 - c)\,C_2(\varepsilon_1, m)$. The theoretical local slope is

$$d_2(\varepsilon, m) = \frac{\ln[C_2(\varepsilon_2, m)] - \ln[C_2(\varepsilon_1, m)]}{\ln \varepsilon_2 - \ln \varepsilon_1} = \ln \beta / \ln \alpha \tag{A18}$$

whereas the estimated slope will be

$$d'_2(\varepsilon, m) = \frac{\ln[C'_2(\varepsilon_2, m)] - \ln[C'_2(\varepsilon_1, m)]}{\ln \varepsilon_2 - \ln \varepsilon_1} \approx 2\,c / \ln \alpha + \ln \beta / \ln \alpha \tag{A19}$$

where we have considered $\ln(1 \pm c) \approx \pm c$ due to the small value of c. Therefore, the relative error in $d_2(\varepsilon, m)$ is $2\,c / \ln \beta$. For $\beta = 0.9$, the relative error becomes $\approx 20\,c$ which means that a 1% error in $C_2(\varepsilon_2, m)$ can result in an error in $d_2(\varepsilon, m)$ as high as 20%.

3. Real world examples

In this section we present the details of some real world hydrometeorological series, which include rainfall on daily, sub-daily, and monthly timescale (sections 3.1, 3.2, and 3.3, respectively) relative humidity (section 3.4) and streamflow (section 3.5). Summary of this investigation is given in Koutsoyiannis (2006).

3.1 Daily rainfall series

As explained in Koutsoyiannis (2006), the role of rainfall is crucial in investigating chaos in hydrological processes, since rainfall is the input that mobilizes all other hydrological processes in a catchment. Also, in Koutsoyiannis (2006) some arguments that the rainfall process cannot be low-dimensional deterministic are presented, without applying any algorithm to determine dimensions. However, just for demonstration we apply the standard algorithm to some historical rainfall data series. Several such series were examined and the results are in all cases similar. Here we present the results for one series, the daily data at the Vakari raingauge, western Greece. This raingauge is located in one of the wettest parts of Greece with 40% rainy days and a mean annual rain depth approaching 1700 mm. (According to the arguments in Koutsoyiannis (2006) the wetter the climate regime the greater is the hope of lower dimensionality of the attractor). More than 31 years or 11 476 daily data values were available. Among these years, the maximum dry spell length is 47 days, that is, 2.5 times smaller that that of the Athens raingauge discussed in Koutsoyiannis (2006). The mean, standard deviation and coefficient of skewness of the data record are 4.59 mm, 11.90 mm and 4.59, respectively. Had the zero values been excluded from the record, these statistics would be 11.38, 16.55, and 2.96, respectively. In any case, the skewness is very high and the distribution is J-shaped. The lag-one autocorrelation of the series is 0.35, which means that a delay $\tau = 1$ would suffice. Plots of the delay representation of the series in two and three dimensions are shown in Figure 2 in Koutsoyiannis (2006). However, for the application of the Grassberger-Procaccia algorithm we chose a much higher (and thus safer) value, $\tau = 12$, which we located as the position where the autocorrelation function has its first minimum.

In Figure A1 we have plotted the correlation sums $C_2(\varepsilon, m)$ (upper panel) and their local slopes $d_2(\varepsilon, m)$ (lower panel) versus scale ε for embedding dimensions $m = 1$ to 8 calculated from the this daily rainfall series. As expected due to the presence of zeros in the data series, the local slopes for all embedding dimensions become zero for small scales ($\varepsilon \leq 0.0004$). Thus, this figure says nothing about the capacity dimension of the "attractor" of the rainfall process. If we incorrectly ignored the small scales and instead chose scales in the region 0.01-0.1, we would come up with small positive dimensions, not exceeding 1.5 even for embedding dimensions 8. If we also continued the plots for embedding dimensions 10, 20, 30 and so on, totally ignoring the astronomical number of data points required to do estimations in these dimensions, it is very probable that we would conclude that there is a low dimensional chaotic attractor here with dimension 1.5. This, however, would be a totally erroneous result.

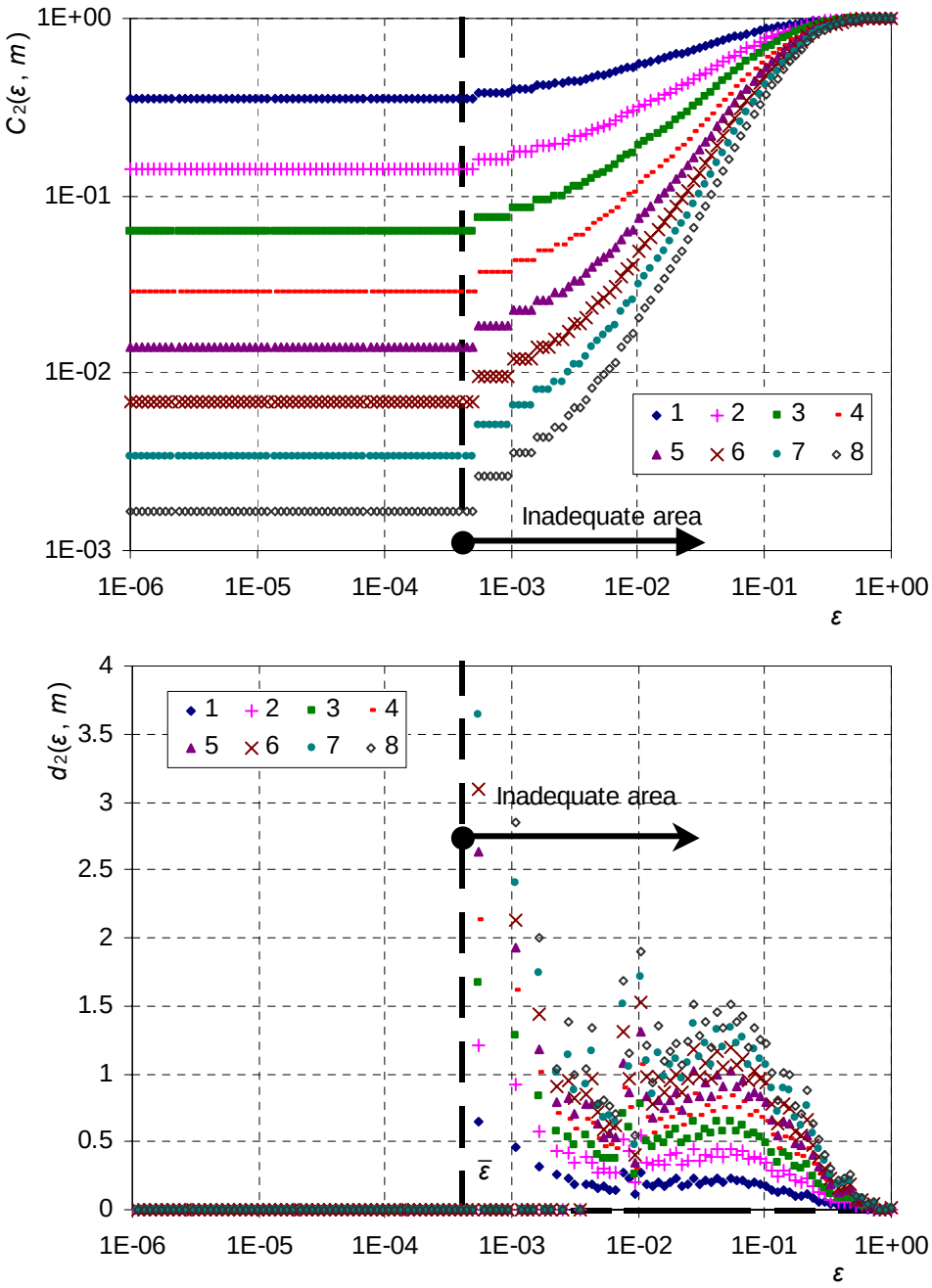

Figure A1 Correlation sums $C_2(\varepsilon, m)$ (upper panel) and their local slopes $d_2(\varepsilon, m)$ (lower panel) vs. scale ε for embedding dimensions m = 1 to 8 calculated from the daily rainfall series at the Vakari raingauge.

It is interesting to see what happens with this data series if we exclude zero data values and apply the algorithm due to Graf von Hardenberg *et al.* (1997b). This is shown in Figure A2, where again we observe that the local slopes $d_2(\varepsilon, m)$ become zero for small scales. In this case, this is the result of round-off errors in the data values, rather than a theoretically consistent result. Specifically, 5% of the values have been rounded to 0.1 mm (which is the limit of the measuring device), 4% as 0.2 mm, 3% as 0.3 mm and so on. This is equivalent to having

nonzero probabilities of occurrence of these values, which in turn results in zero slope of the correlation sum. The main difference of Figure A2 from Figure A1 is that even for large scales the local slopes tend to more reasonable values, i.e., to about 0.7 for m = 1, 1.4 for m = 2, etc.

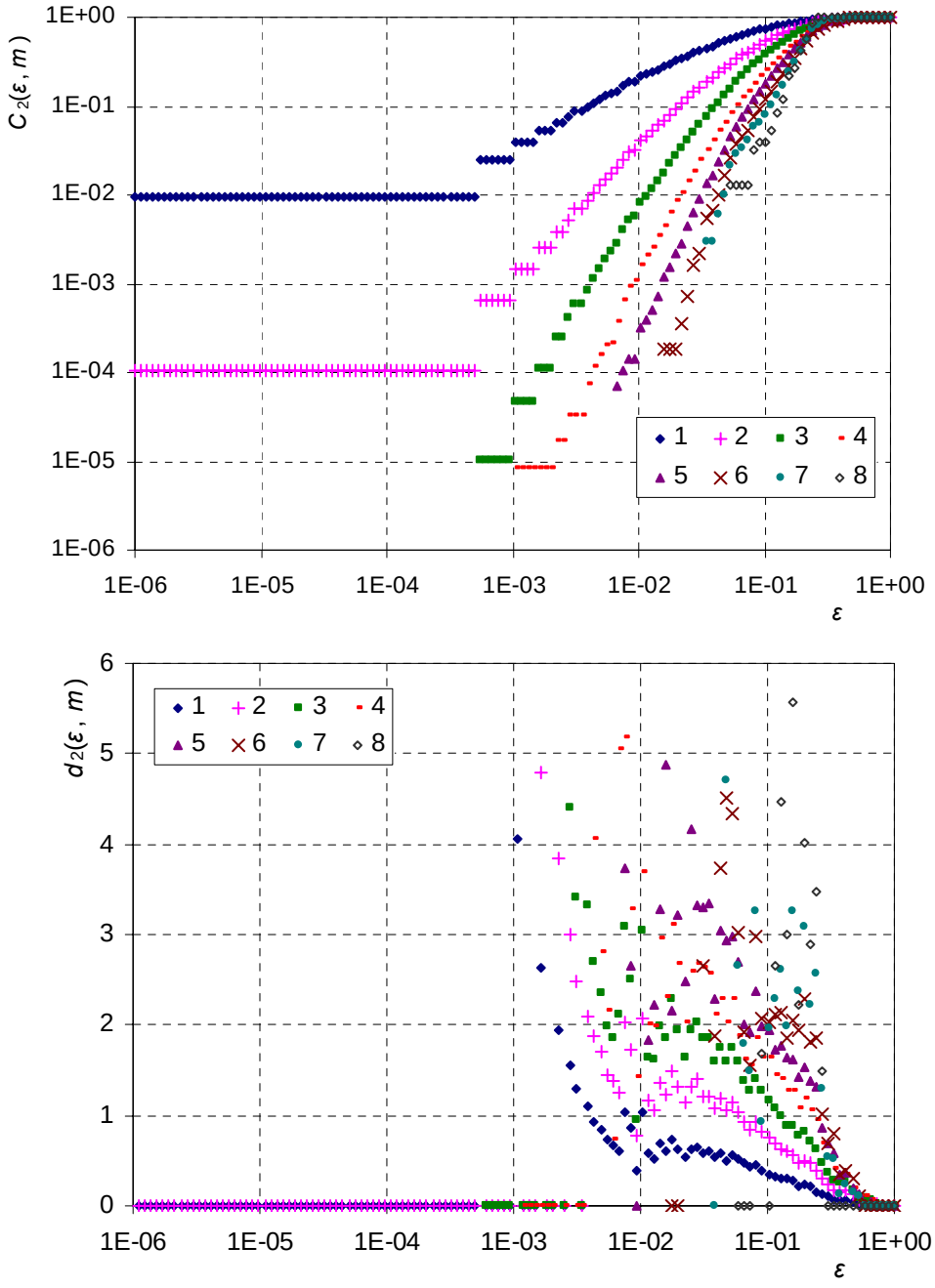

Figure A2 Correlation sums $C_2(\varepsilon, m)$ (upper panel) and their local slopes $d_2(\varepsilon, m)$ (lower panel) vs. scale ε for embedding dimensions m = 1 to 8 calculated from the same daily rainfall series as in Figure A1 but excluding points with zero values.

To minimize the effect of round-off errors we also performed another application of the algorithm by Graf von Hardenberg *et al.* (1997b) excluding data values that are less than 2 mm. In this case the sample size becomes too low to allow for any accurate estimation but clearly shows that the correlation dimension $D_2(m)$ tends to the embedding dimension m, which means that the time series has a stochastic character.

3.2 Storm data

If the presence of zeros in a rainfall time series is a strong obstacle to analyzing the presence of chaos, one may think that going to a much finer timescale and limiting the analysis strictly to a rainy period (a single storm) one could find the deterministic chaos. The idea of a deterministic (meaning low dimensional?) evolution of a storm has been favoured long before hydrologists became involved with chaos. For example, Eagleson (1970, p. 184) states "The spacing and sizing of individual events in the sequence is probabilistic, while the internal structure of a given storm may be largely deterministic".

To explore this idea we used a storm time series measured with high temporal resolution. This data set corresponds to one of several storms that were measured by the Hydrometeorology Laboratory at the University of Iowa using devices that are capable of high sampling rates (Georgakakos *et al.*, 1994). The data is available on the Internet from ftp.iihr.uiowa.edu. Specifically, the data set used is that of the event labeled Rain 1, which occurred during 2-3 December 1990.

The duration of this storm was almost 27 h and the rain depth was measured every 10 s, so that the data set contains 9679 data points. The total depth is 104.9 mm, and the mean, maximum and minimum 10-second intensity are 3.89, 118.74, and 0.07 mm/h, respectively. The standard deviation of the 10-second intensities is 6.16 mm/h (1.58 times the mean) and their coefficient of skewness is 4.83. The distribution function is J-shaped and the gamma distribution function with a shape parameter 0.40 gives an acceptable fit to the data series. The autocorrelation is very high. For lags 1, 100 and 500 is 0.88, 0.48 and 0.15, respectively, and only at lag 850 becomes zero. For high frequencies ($> 4\times10^{-3}$ cycles per second) the power spectrum is approximately a power function of frequency with an exponent 1.63 (estimated by Georgakakos *et al.*, 1994).

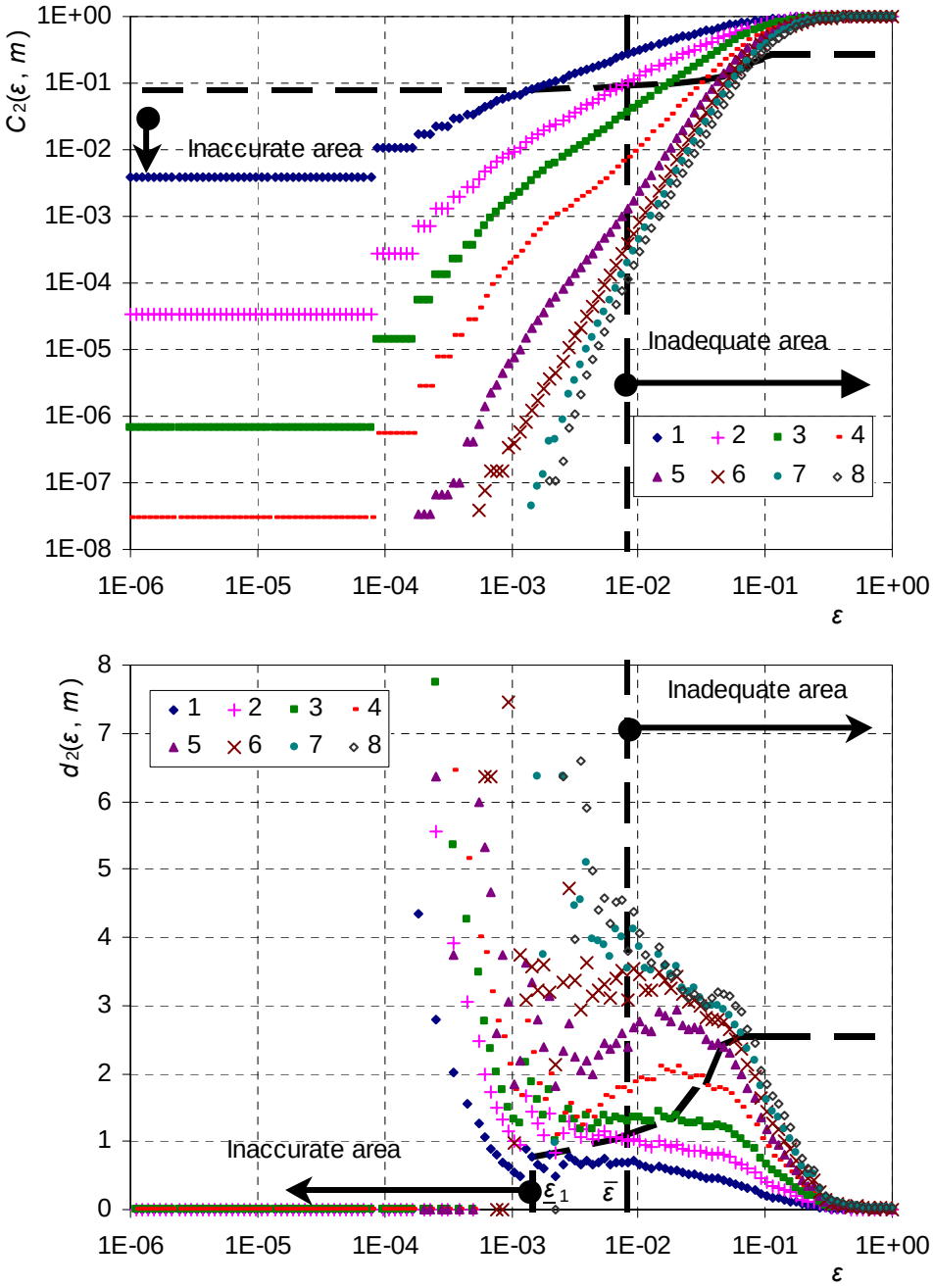

Figure A3 Correlation sums $C_2(\varepsilon, m)$ (upper panel) and their local slopes $d_2(\varepsilon, m)$ (lower panel) vs. scale ε for embedding dimensions m = 1 to 8 calculated from the fine timescale rainfall series at Iowa.

The correlation sums $C_2(\varepsilon, m)$ of this time series for τ = 500 and their local slopes $d_2(\varepsilon, m)$ are plotted in Figure A3 versus scale ε for embedding dimensions m = 1 to 8. Again here we observe zero slopes for low scales. These again are due to round-off errors that artificially result in equal values: for example 217 values are 0.09 mm/h and 169 are 0.08 mm/h. If we ignore the regions with zero slopes, and apply the statistical reasoning exhibited in Koutsoyiannis (2006), we find that for the plot of m = 1 the upper limit for adequate estimations is $\bar{\varepsilon}$

= 0.008 and the lower limit for accurate estimations is $\underline{\varepsilon}_1$ = 0.0014. For m = 2, we find from (21) (Koutsoyiannis, 2006) that $\underline{\varepsilon}_2$ = 0.0072 < $\overline{\varepsilon}$, whereas for all greater m, $\underline{\varepsilon}_m$ > $\overline{\varepsilon}$. Thus, $D_2(m)$ can be estimated only for m = 1 and 2, and the estimated $D_2(1)$ = 0.69 and $D_2(2)$ = 1.00. Given that the shape parameter of the gamma distribution is 0.40, the expected values for an entirely random series are 0.80 and 1.60 for m = 1 and 2 respectively. In any case, these results do not support nor prohibit the existence of low-dimensional deterministic dynamics.

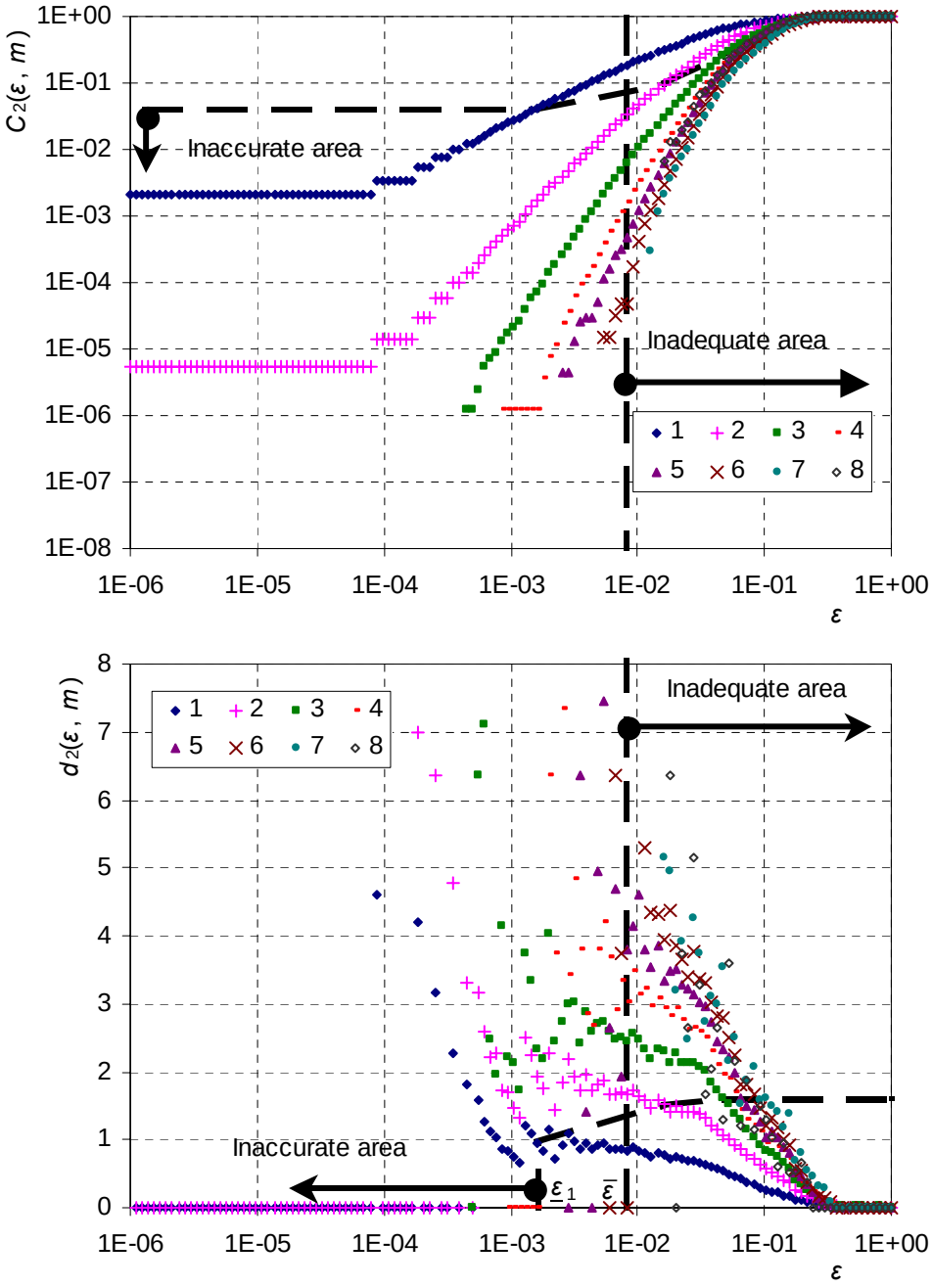

Figure A4 Correlation sums $C_2(\varepsilon, m)$ (upper panel) and their local slopes $d_2(\varepsilon, m)$ (lower panel) vs. scale ε for embedding dimensions m = 1 to 8 calculated from the fine timescale rainfall same series as in Figure A3 but excluding points having at least one coordinate smaller than 0.01.

As an additional analysis, we applied the Graf von Hardenberg *et al.* (1997b) algorithm excluding data values smaller than 1% of the maximum value and plotted the resulting correlation sums and local slopes in Figure A4. Now it can be observed that $D_2(1) = 1$ and for higher dimensions, although no accurate estimations can be obtained, it is apparent the tendency that $D_2(m) = m$, which indicates the absence of chaotic behaviour.

3.3 Monthly rainfall series

It has been found that many systems are composed of a huge number of internal microscopic degrees of freedom, but nevertheless produce signals which are found to be low dimensional (Kantz & Schreiber, 1997, p. 34). The coupling between the different degrees of freedom and an external field of some kind, lead to collective behaviour which is low dimensional. The reason is that most degrees of freedom are either not excited at all or "slaved" (Kantz & Schreiber, 1997, p. 239).

By analogy, it may be useful to study a hydrological process on a coarse timescale and try to identify chaos there. Even if the system on a fine timescale appears random, one may think of some collective behaviour on the coarser timescale, which could result in a low-dimensional attractor.

Here we present the results for one series on a coarse timescale, the monthly rainfall in at the station of the National Observatory in Athens, which is the longest rainfall record in Greece (see Koutsoyiannis & Baloutsos, 2000). This corresponds to a dry climate with about 400 mm annual rainfall; in 9% of the months the rainfall is zero. More than 132 years or 1586 monthly data values were available (August 1859 to September 1991). The mean, standard deviation and coefficient of skewness of the data record are 32.9 mm, 36.0 mm and 1.75, respectively. Had the zero values been excluded from the record, these statistics would be 36.4, 36.2, and 1.70, respectively. Despite the large skewness, the distribution is bell-shaped. The autocorrelation coefficient of the series is 0.32 for lag one and decays quickly, so that it becomes negative for lag three.

The correlation sums and the local slopes of this series, excluding zero points and using delay $\tau = 1$, are plotted in Figure A5 versus scale ε for embedding dimensions $m = 1$ to 8. Due to the small record size only the estimate of $D_2(1)$ is accurate (as verified from the graphical application of the procedure described Koutsoyiannis (2006) shown in Figure A5) and is about 1. For higher dimensions no accurate estimations can be obtained, but again the tendency is that $D_2(m) = m$, which does not signify a chaotic behaviour.

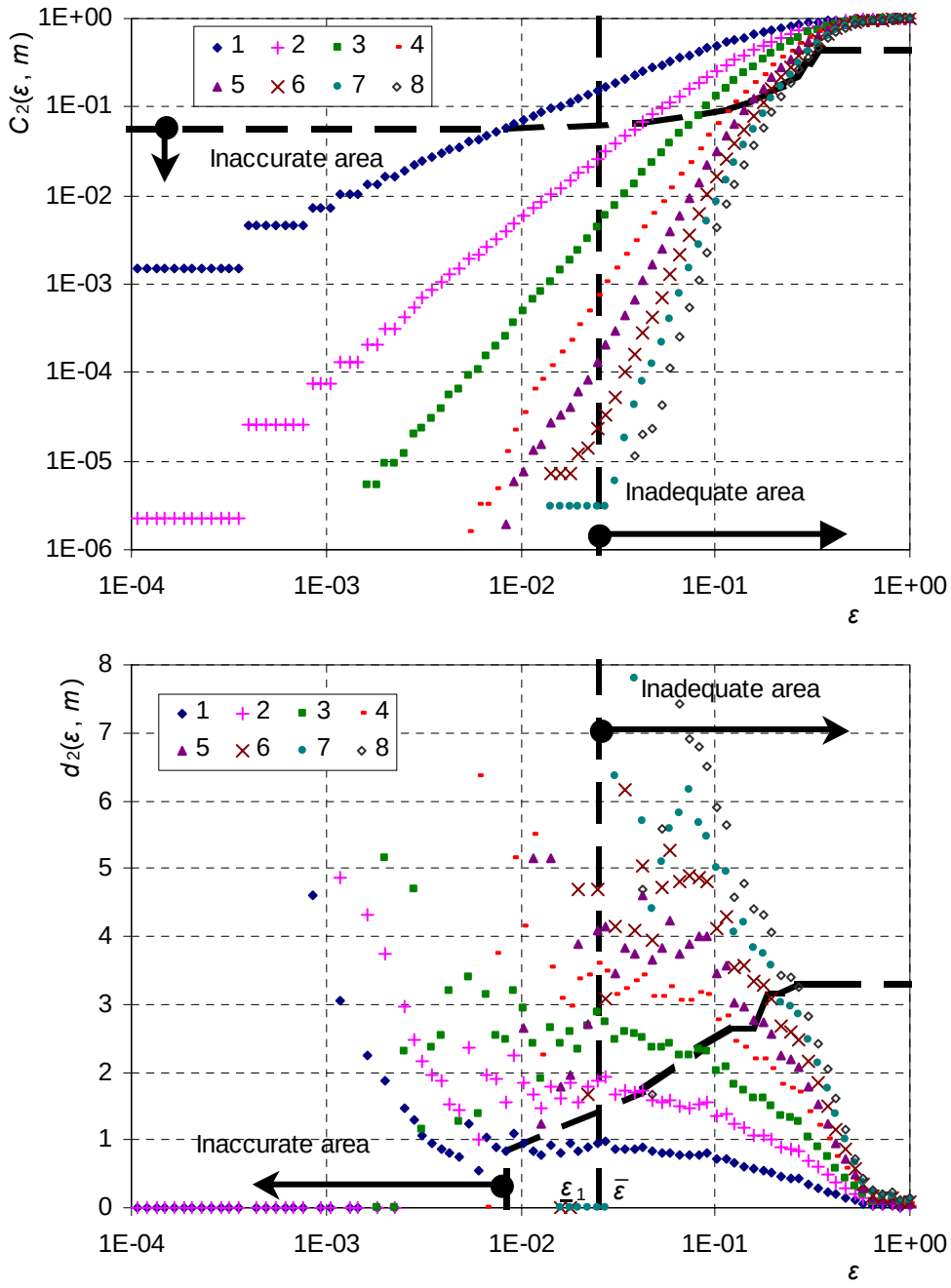

Figure A5 Correlation sums $C_2(\varepsilon, m)$ (upper panel) and their local slopes $d_2(\varepsilon, m)$ (lower panel) vs. scale ε for embedding dimensions m = 1 to 8 calculated from the monthly rainfall series at Athens excluding zero points.

3.4 Relative humidity series

Since we found difficulties in identifying chaos in rainfall on all timescales, it could be a good idea to move to another related process in the direction of meteorology. The meteorological variable most closely related to rainfall is the relative humidity since when it rains, it approaches saturation (i.e., the value 100%). The data series we used is the relative humidity

of the period 1 December 1998 to 4 February 2001 on hourly timescale (18 888 data values) and comes from the meteorological station of the National Technical University in Athens (available on the Internet at www.itia.ntua.gr/meteo/); a few missing values were filled in by linear interpolation in time. Obviously, the relative humidity series is totally free from zeros and intermittency, which makes its study easier. The mean, standard deviation and coefficient of skewness of the data record are 60.2%, 17.2% and –0.26, respectively, whereas the minimum and maximum values are 12.3% and 99.0%. The distribution is bell-shaped. The autocorrelation coefficient of the series is as high as 0.97 for lag one and decays slowly, so that it becomes smaller than 1/e only for lag 108.

The correlation sums $C_2(\varepsilon, m)$ of this time series for $\tau = 108$ and their local slopes $d_2(\varepsilon, m)$ are plotted in Figure A6 versus scale ε for embedding dimensions $m = 1$ to 8. We observe on the plots of $m = 1$ that a long scaling area appears between $\overline{\varepsilon} = 0.08$ and $\underline{\varepsilon}_1 = 0.00092$. Thus, $\underline{\varepsilon}_m < \overline{\varepsilon}$, for $m \le 4$, as shown graphically in Figure A6, which means that $D_2(m)$ can be estimated accurately for $m = 1$ to 4. The estimated values are $D_2(m) = m$, a result that again does not allow any hope for low-dimensional determinism.

3.5 Daily streamflow series

Finally, we will study the most representative hydrological process using a daily streamflow series of the Pinios River, central-eastern Greece, at the Ali Efenti gauge. The data series extends through the period 3 January 1972 to 18 March 1998 (8 246 data values of which 1435 were missing data that were left unfilled). As explained Koutsoyiannis (2006), a streamflow series must be regarded as intermittent even if it is free from zeros. The mean, standard deviation and coefficient of skewness of the data record are 39.6 m^3/s, 56.5 m^3/s and 3.46, respectively, whereas the minimum and maximum values are 1.0 m^3/s and 553.5 m^3/s. The distribution is very asymmetric yet bell-shaped. The autocorrelation coefficient of the series is as high as 0.86 for lag one and decays slowly, so that it becomes zero only for lag 94.

The correlation sums $C_2(\varepsilon, m)$ of this time series for $\tau = 94$ and their local slopes $d_2(\varepsilon, m)$ are plotted in Figure A7 versus scale ε for embedding dimensions $m = 1$ to 8. We observe on the plots of $m = 1$ that a scaling area appears between $\overline{\varepsilon} = 0.06$ and $\underline{\varepsilon}_1 = 0.001$, whereas for all other m, $\underline{\varepsilon}_m > \overline{\varepsilon}$, which means that an accurate estimation of $D_2(m)$ is possible only for $m = 1$; this is $D_2(1) \approx 1$. For higher embedding dimensions m, a tendency appears for $D_2(m)$ increasing with m, which again does not indicate a chaotic behavior.

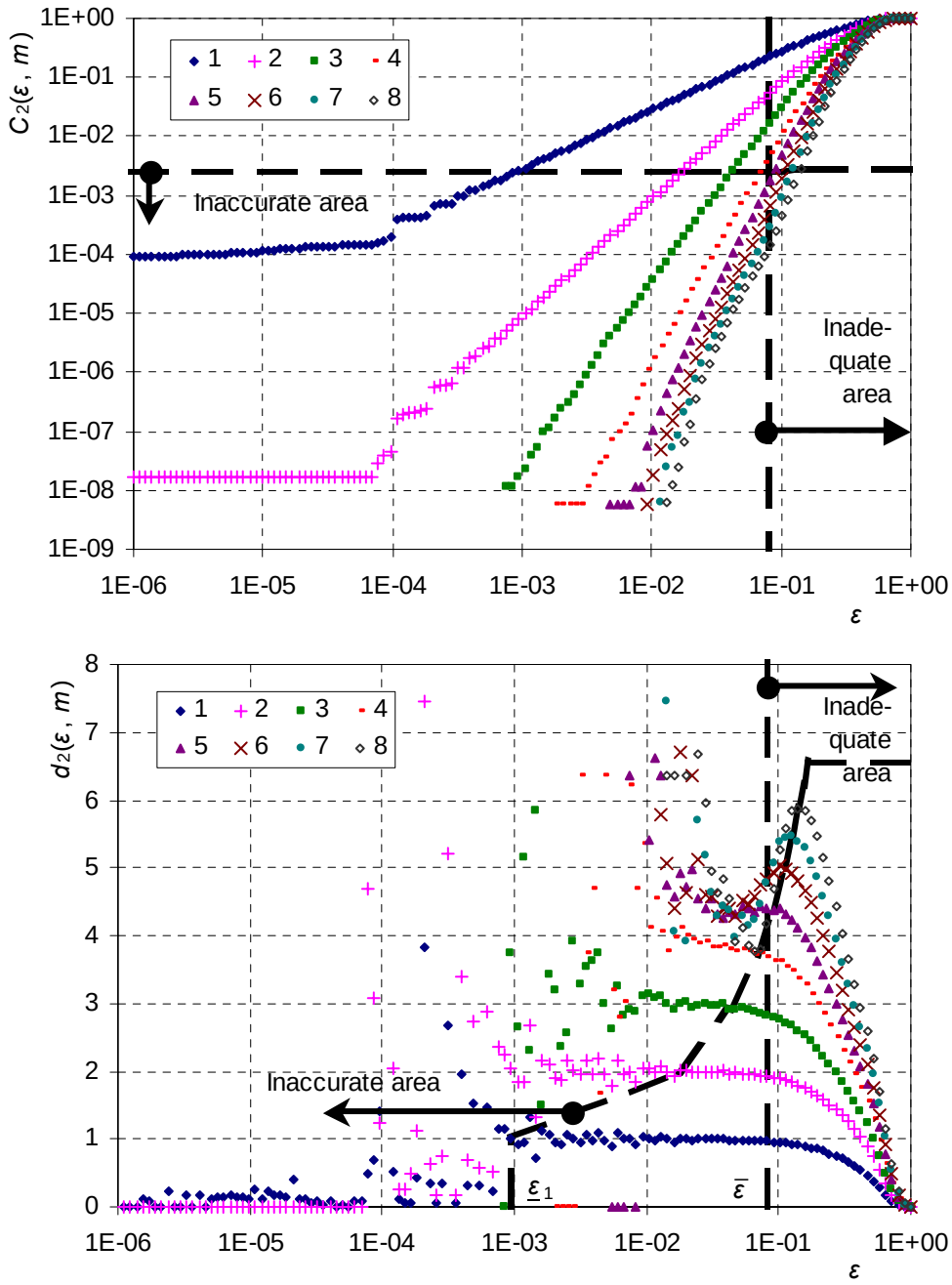

Figure A6 Correlation sums $C_2(\varepsilon, m)$ (upper panel) and their local slopes $d_2(\varepsilon, m)$ (lower panel) vs. scale ε for embedding dimensions m = 1 to 8 calculated from the relative humidity series at Athens.

References

Eagleson, P. S. (1970) *Dynamic Hydrology*, McGraw-Hill.

Georgakakos, K. P., Carsteanu, A. A., Sturdevant, P. L., & Cramer, J. A. (1994) Observation and analysis of Midwestern rain rates, *J. Appl. Meteorol.*, 33, 1433-1444.

Graf von Hardenberg, J., Paparella, F., Platt, N., Provenzale, A., Spiegel, E. A., & Tesser, C. (1997b) Missing motor of on-off intermittency, Physical Review E, 55(1), 58-64.

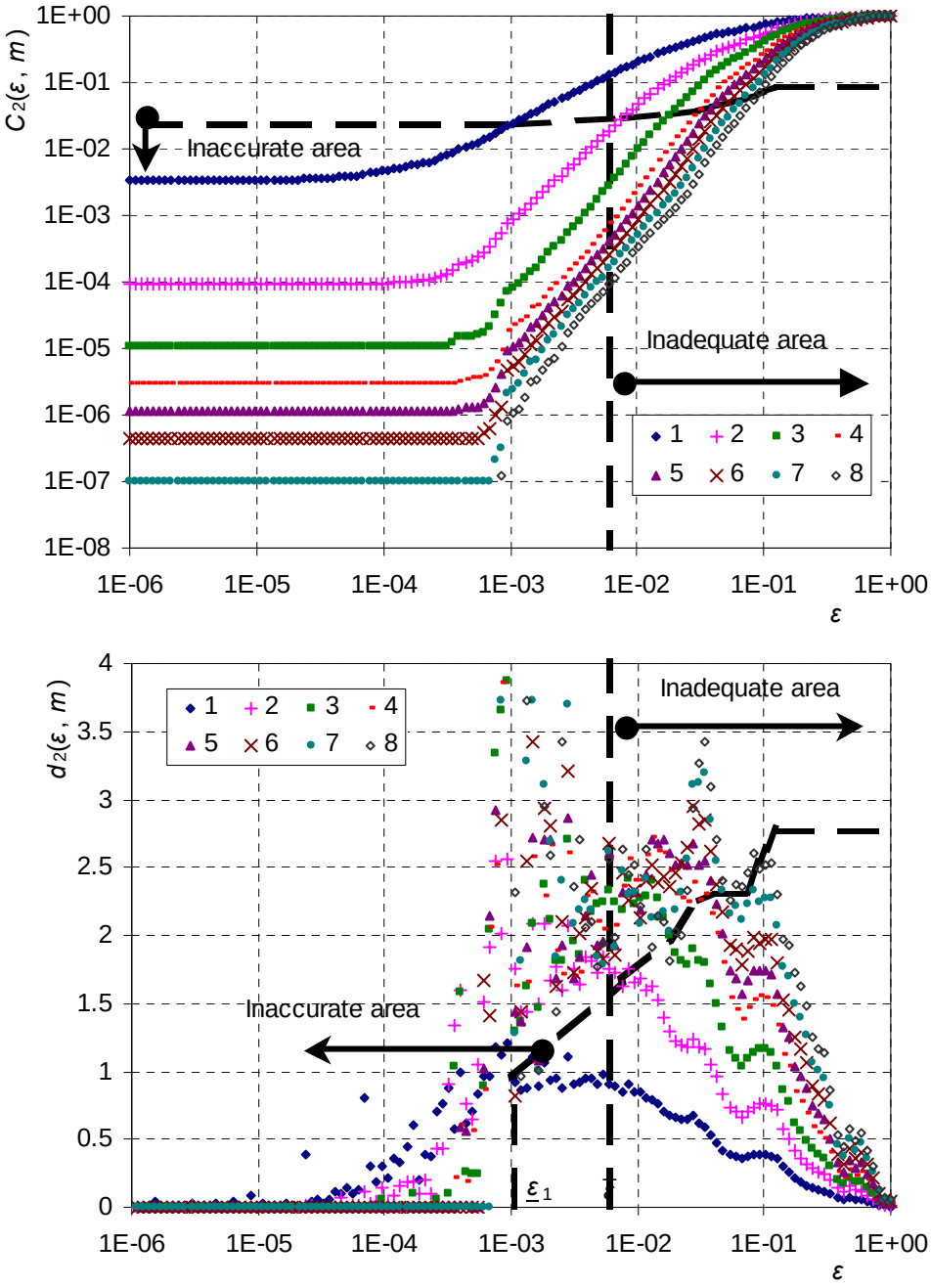

Figure A7 Correlation sums $C_2(\varepsilon, m)$ (upper panel) and their local slopes $d_2(\varepsilon, m)$ (lower panel) vs. scale ε for embedding dimensions m = 1 to 8 calculated from the discharge series at Ali Efenti gauge at Pinios River.

Kantz, H., & Schreiber, T. (1997) *Nonlinear Time Series Analysis*, Cambridge University Press, Cambridge.

Koutsoyiannis, D. (2006) On the quest for chaotic attractors in hydrological processes, Hydrological Sciences Journal (under review).

Koutsoyiannis, D., & Baloutsos, G. (2000) Analysis of a long record of annual maximum rainfall in Athens, Greece, and design rainfall inferences, *Natural Hazards,* 22(1), 31-51.